

# Chapter 29

## Integrated In Situ Investigations for the Restoration: The Case of *Regio VIII* in Pompeii

Nicola Masini, Maria Sileo, Giovanni Leucci, Francesco Soldovieri, Antonio D'Antonio, Lara de Giorgi, Antonio Pecci, and Manuela Scavone

**Abstract** This chapter presents the study case of the integration of noninvasive in situ investigation methods able to provide information useful to survey and characterize the state of decay of some masonry walls and frescoes in two blocks (*insulae*) of the *Regio VIII* in Pompeii. The integrated investigations demonstrated the complementarity of ground-penetrating radar (GPR), seismic tomography, and infrared thermography (IRT) for the diagnosis of the state of conservation and the restoration of structures and surfaces of archaeological monuments. The investigation was very useful in planning the restoration work.

**Keywords** Pompeii • Restoration • Non invasive in situ investigations • GPR • Infrared thermography • Seismic tomography

---

N. Masini (✉) • M. Sileo • A. D'Antonio • A. Pecci • M. Scavone  
CNR-IBAM Institute for Archaeological and Monumental Heritage,  
C. da Santa Loja, 85050, Tito Scalo, Potenza, Italy  
e-mail: [n.masini@ibam.cnr.it](mailto:n.masini@ibam.cnr.it); [m.sileo@ibam.cnr.it](mailto:m.sileo@ibam.cnr.it); [a.dantonio@ibam.cnr.it](mailto:a.dantonio@ibam.cnr.it);  
[m.scavone@ibam.cnr.it](mailto:m.scavone@ibam.cnr.it)

G. Leucci • L. de Giorgi  
Institute of Archaeological and Monumental Heritage, CNR (National Research Council)-IBAM  
(Italy), Lecce, Italy  
e-mail: [g.leucci@ibam.cnr.it](mailto:g.leucci@ibam.cnr.it); [l.degiorgi@ibam.cnr.it](mailto:l.degiorgi@ibam.cnr.it)

F. Soldovieri  
Institute for Electromagnetic Sensing of the Environment (CNR-IREA),  
Via Diocleziano 328, 80124, Napoli, Italy  
e-mail: [soldovieri.f@irea.cnr.it](mailto:soldovieri.f@irea.cnr.it)

## 29.1 Introduction

Correct planning of the restoration interventions of architectural and archaeological monuments requires a detailed study of building techniques and materials, the mapping of decay patterns, the localization of damage, and the identification of their causes.

In particular, the detection and mapping of voids and cracks in the masonry structures and plaster detachments and alterations are crucial (1) to verify the stability of load-bearing structures and (2) to evaluate the state of conservation of architectural and painting surfaces, respectively.

In the past, such information was obtained by means of coring of samples and other destructive inspections. Nowadays, increased awareness of the historical and artistic value and brittleness of artifacts mandates the use of noninvasive investigations. This provision is in agreement with the first axiom of the Theory of Restoration of Cesari Brandi, which states that “only the material form of the work of art is restored”. . . because “the material ensures the transmission of the image to the future” (Brandi 1963).

In the past two decades, development of the technologies associated with geophysical methods, improvement of performance and resolution of sensors and devices, and the increasing availability of user-friendly software for data analysis, processing, and interpretation have led to an increasing interest in the use of in situ nondestructive testing (NDT). In this way, it is possible to give an answer to the several issues related to the structural stability assessment and the analysis (qualitative and quantitative) of weathering of building materials, by respecting the value and fragility of the artifact. With particular reference to structural restoration, as declared by ICOMOS (2003) the investigations should be aimed not only to “safety evaluation” but also to “understanding of the significance of the structure.”

The available NDT techniques are based on different working principles. Their choice for studying a particular conservation problem depends on the physical properties of the building materials. In particular, in the case of masonry structures, the choice of the method to be used depends on these factors:

1. The characteristics of the constituents of building materials such as bricks (fired or sun-dried), stone (sandstone, limestone, etc.), and mortar (gypsum, lime, pozzolanic, ordinary Portland cement)
2. The kind of decay to be identified and mapped (fractures, moisture content, plaster detachments)
3. The depth of investigation and the size (which dictates the spatial resolution) of the target (crack size, plaster/fresco thickness, air thickness between plaster and wall)

A few items of this information, such as those related to the material constituents, can be achieved by geochemical and petrographic analyses in the laboratory. Other information related to decay characterization can also be obtained by in situ investigation techniques, such as ground-penetrating radar (GPR), seismic

tomography, and infrared thermography (IRT), which prove to be effective and complementary for all the building elements of cultural interest (from the wall to plaster).

For sake of brevity, we only provide the main characteristics from the theoretical and application aspects of these methods, referring the reader, for a more comprehensive discussion, to the chapters in this volume by Persico and Sato (2016), Leucci (2016), and Dumoulin (2016), respectively.

### **29.1.1 Ground-Penetrating Radar**

Ground-penetrating radar (GPR) exploits the capability of electromagnetic waves (EM) to propagate in a medium (such as masonry structures, concrete beams, fresco) with the aim to identify the inner reflections in correspondence of interfaces separating media with different electromagnetic properties (dielectric permittivity, electrical conductivity, and magnetic permeability) (Persico 2014). The GPR equipment exploits an antenna pair in which the transmitting antenna sends short EM pulses into the subsurface and the receiving antenna collects the backscattered radar echoes. The nominal frequency of the antenna is typically in the range of 800–2000 MHz for investigating media ranging from a wall 1 m thick to a plaster layer 5–10 cm thick.

To provide quantitative information on features of cultural interest (masonry or plaster thickness) and decay pathologies (void and crack size), the crucial step is the estimation of subsurface propagation velocity (Persico 2014). This estimated EM wave velocity permits the conversion of the time into depth along the radar profile.

The result of GPR data processing allows identifying interfaces between different constructive layers (which typically could be found in the ancient Roman walls in *opus coementicium*) or local reflectors referable to iron bars (which typically are inserted during consolidation interventions), voids, or fractures. In addition, the presence of moisture in the medium is detected by determining the increase of conductivity that causes a high absorption of the EM waves. To facilitate the interpretation of the reconstructed images compared to standard data processing, an effective approach is based on the use of microwave tomography able to obtain high-resolution images useful for the detection and the shape reconstruction of localized features both for archaeological prospection (Soldovieri and Orlando 2009) and for historical monument investigations (Leucci et al. 2011).

The various modalities of three-dimensional (3D) GPR result in visualization that can help us in interpreting those anomalies referring to strong reflectors (e.g., relating to the presence of large inhomogeneities and voids), but at the same time it is not possible to see ‘subtle’ anomalies attributable to weak reflectors, whose nature is more easily understood by looking at the radargrams. This behavior occurred during the GPR investigation of the columns of a Romanesque rose window in Apulia (Masini et al. 2007). The radargrams allowed us to understand how the columns were joined with the central oculus of the rose window: in some cases with iron belts

and molten lead, in other cases just inserting the columns inside hollow cylindrical elements. This information made possible to reconstruct the relative chronology of building phases and to suggest the most effective measure of reinforcement.

In the field of architectural heritage, GPR surveys have been performed for detecting the constructive characteristics of masonry structures (Maierhofer and Leipold 2001; Ranalli et al. 2004; Binda et al. 2005; Masini et al. 2010a) and for investigating the foundation subsoil and discovering archaeological remains, also in conjunction with other geophysical, physical, and biological techniques (Cardarelli et al. 2002; Cataldo et al. 2005; Nuzzo et al. 2007).

In particular, Ranalli et al. (2004) applied GPR for evaluating the state of conservation of the facade of a medieval church, estimating the thickness of its walls, and characterizing the forms and deterioration of masonry composed by external ashlar and the rubble core nucleus. Leucci et al. (2007) detected and assessed fractures in marble columns in the crypt of Otranto Cathedral by GPR in reflection mode. In Spain, Perez-Gracia et al. (2008) detected the point of contact between the Roman remains and the materials used in later restorations in the Theatre of Sagunto and Solla et al. by integrating GPR and simulation of FDTD (finite-difference time-domain) models achieved to identify the ancient profile of a Roman bridge.

### **29.1.2 Seismic Methods**

The seismic method exploits seismic waves, created by a controlled source, that propagate through the subsurface. Seismic methods (sonic and ultrasonic) proved to be effective in providing information useful for the evaluation of the state of conservation of masonry structures, stone decorative elements, stuccoes, and plaster (Binda et al. 2003; Cosentino et al. 2009; Leucci et al. 2012; see also Chap. 8 by Leucci, this volume). The analysis of propagation characteristics of seismic waves, the measurement of the two travel times, and the computation of the two-dimensional (2D) or three-dimensional (3D) velocity distribution allow providing indirect information on the presence of inhomogeneities, cracks, and fractures.

Seismic waves are classified into two groups: surface waves and body waves. The first can propagate along the boundary of the solid. The second propagates through the volume of an elastic medium in two different ways: (i) by compression and dilatation uniaxial strains in the direction of wave travel (the so-called compressional waves or longitudinal or primary or P-waves); or (ii) by a pure shear strain in a direction perpendicular to the direction of wave travel (the so-called shear waves or transverse or secondary or S-waves). Seismic tomography proved to be the most effective way to provide information on constructive characteristics of buildings and artifacts from the elastic waves (sonic or ultrasonic) because it exploits data acquired not only in the direct mode but also along paths that are not perpendicular to the wall surfaces. The resolution achieved by seismic tomography depends on the wavelength. Layers or objects can be discerned when their thickness is less than one fourth the wavelength ( $\lambda$ ). In many cases, it is still possible to discriminate two

targets also with thickness less than  $1/4 \lambda$ , thus allowing us to investigate a large variety of decay patterns and constructive characteristics difficult to see from GPR. This was the case of Tricarico Cathedral where the integration of GPR and seismic tomography allowed evaluation of the size and severity of some fractures visible on the outer sides of the pillars as well as understanding that the pillars were affected by a crushing phenomenon (Leucci et al. 2011).

Finally, seismic tomography can be employed for applications more focused on the mechanical behavior analysis of historical masonry structures. This kind of application makes seismic tomography a routine technique in the field of restoration and retrofitting of monuments and built heritage, especially when it is used in a complementary way with in situ tests aimed at determining the stress, deformability, and resistance features of masonry. This application occurs in the integration of seismic tomography with the flat jack test, performed by making a cut to a uniform depth into the mortar courses and inserting the flat jack or a couple of jacks, which are pressurized to the desired level. In this context, the reader is referred to Binda et al. (2003), who investigated the pillars of the Cathedral of Noto using sonic tomography and the flat jack test, and to Saisi et al. (2015), who assessed the state of preservation of Gabbia Tower in Mantia after an earthquake by integrating sonic tomography with flat jack tests and ambient vibration tests.

### 29.1.3 *Infrared Thermography*

Infrared thermography (IRT) is a remote sensing technique capable of acquiring infrared radiation emitted by objects above 0 K. By means of the Stefan–Boltzmann law, the energy can be measured in terms of temperature by using a suitable IR device. The energy emitted by the surface depends on a large number of properties such as (1) the spectral property (emissivity, reflection), (2) the thermal property (conductivity, specific heat, diffusivity), and (3) other physical properties of the underlying material such as water content, porosity, and density (for additional detail on IRT in relationship to the thermo-optical properties of materials, see the chapter by Dumoulin (2016) in this volume). Accordingly, the interpretation of IR images is not an easy task. However, for the inspection and diagnosis of historic buildings IRT is generally used to map moisture, detect shallow subsurface voids and defects, and evaluate the conservation treatments in a qualitative way.

IRT surveys can be carried out in two ways depending on the source that creates the heat transfer process, which can be (1) passive, when the source of the thermal wave is natural, or (2) active, when an artificial source is used to create the thermal excitation of the object to be investigated. The active technique can be used in four ways: (i) graduated heating thermography; (ii) lock-in thermography; (iii) pulsed thermography (PT); or (iv) pulsed phase infrared thermography (PPT).

(i) In graduated heating thermography, surface temperature is measured during heating. (ii) Lock-in thermography, based on the concept of the thermal wave, consists of introducing periodically modulated heat into the specimen or object and monitoring the periodic temperature modulation phase, referred to the modulated

heat supply. (iii) PT consists of recording temperature decrease after the specimen is heated briefly. (iv) PPT, which is based on the Fourier transform, combines the advantages of both pulsed infrared thermography and lock-in thermography.

In the field of artistic and architectural restoration, the passive technique is mostly used for various purposes such as (i) the detection of shallow subsurface voids and defects of architectural surfaces (Inagaki et al. 1999; Maierhofer et al. 2003), (ii) to map moisture (Grinzato et al. 2002a), and (iii) to evaluate conservation treatments (Avdelidis and Moropoulou 2004). The integrated use of different active techniques with or without passive thermography is also applied for decay analysis of outdoor cultural heritage such as the murals of the monastery of Molybdoskepastos, whose decay has been evaluated by using graduated heating thermography, lock-in thermography, and PPT by Kordatos et al. (2013).

For operational use, the active approach is usually applied to small areas (e.g., mosaics, specimens in laboratory) when the controlled thermal excitation is feasible.

Passive thermography is mainly employed for large areas to be investigated (e.g., architectural surfaces, mural paintings). The limits in terms of discriminability of thermal anomalies generally make necessary the use of the following:

- Other noninvasive in situ investigations as done by Moropoulou et al. (2013) for monitoring cleaning interventions on architectural surfaces of medieval fortifications in Rhodes, and Nuzzo et al. (2010) for detecting cracks and conservation treatments in the Romanesque rose window of Troia (Southern Italy)
- Different thermographic equipment and spectral bands as done by Grinzato et al. (2002b) to identify hidden structures, evaluate the adhesion of frescoes, and map cracks in the Chapel of Scrovegni painted by Giotto between 1303 and 1305;
- New data processing approaches such as visual analytics to extract from multitemporal IRT data the decay patterns of the calcarenite architectural facade of the Cathedral of Matera (Danese et al. 2010).

### **29.1.4 Integration**

The usefulness of the results achievable by GPR, seismic, and IRT methods for the knowledge and assessment of the state of conservation of cultural heritage depends on the quality of the feedback between scientists (experts in noninvasive diagnostics) and end-users (archaeologists, architects, conservators). The quality of this feedback entails the end-user capability of transforming the diagnostics outcomes into information easily interpretable for multiple purposes such as mapping, monitoring, and assessing decay pathologies, planning conservation, and retrofitting interventions.

From our experience (Masini et al. 2010b; Masini et al. 2013) in the field of cultural heritage and namely the conservation of monuments, we noted that there is a relevant gap in the information sharing/transfer between professionals (geophysicists/physicists/engineers) and end-users (conservators/historians/architects).

This gap is generally caused by the difficulty in interpreting the results obtained by noninvasive diagnostics in terms of information useful to characterize and monitor the state of conservation (e.g., detection of cracks in the masonry) as well as to improve the historical knowledge of monuments and artifacts (e.g., identification of ancient building elements and phases).

Several experiences suggest an integrated strategy aimed at improving the interpretation of diagnostics and remote sensing by means of the following steps:

- (a) Integration and fusion of in situ noninvasive tests and geophysical methods
- (b) Comparison between direct data (carrots, endoscopic tests, visual inspection) and results from noninvasive tests, including geophysics
- (c) Use of specimens or test beds for the detection of archaeological features and monitoring of monuments and sites
- (d) Augmented reality as a tool for facilitating the interpretation of noninvasive investigations

As examples of the approach (a), the reader is referred to Pérez-Gracia et al. (2013), wherein GPR and seismic tomography were integrated for the physical and geometrical characterization of structural elements of the Mallorca Cathedral. D'Aranno et al. (2015) investigated an ancient Roman wall through high-resolution geomatics, geophysical methods, and chemical analysis: laser scanner surveys allowed analyzing wall geometry and surface, chemical analyses were performed to identify the constitutive material, and GPR provided information on the inner core of the wall. Other examples are in found in Masini et al. (2007) and Moropoulou et al. (2013).

With respect to approach (b), we cite two case studies. One is related to the Cathedral of Matera, where investigations by GPR were aimed at characterizing the inner structure of two pillars by exploiting the available data provided by a coring (Masini et al. 2010a). The second application is related to the Cathedral of Tricarico where an integrated approach-based GPR and sonic prospecting was applied to detect cracks and inhomogeneities in the inner structure of masonry pillars (Leucci et al. 2011). For two pillars of the Tricarico Cathedral, the results have been compared with coring and endoscopy, thus facilitating the interpretation of GPR and sonic tomography on the other pillars of the church. The results of GPR and sonic tomography allowed discovery of the existence of a crushing phenomenon affecting the pillars of the cathedral, thus suggesting the most effective retrofitting solution.

The approach (c) is based on the use of specimens that allows developing reproducible and highly accurate diagnostics methods to be applied for on-site investigations. It could be used (i) for investigations strongly based on one diagnostic test, such as IRT for investigating architectural and painted surfaces or ultrasonic investigations, to evaluate and quantify superficial alterations of natural stone (Meier et al. 2016), or (ii) for applications based on the use of more noninvasive tests such as IRT and GPR for evaluating the state of conservation of frescoes as well of the underlying masonry structure (Carlomagno et al. 2011).

Finally, an example of the approach (d) is given by Gabellone et al. (2013), wherein experienced augmented reality improved the interpretation of GPR prospections carried on the floor and walls of the chapel of the Holy Spirit in Lecce.

In this work, we present the approach used and the obtained results in an investigation campaign in some *insulae* of Region VIII of the Roman town of Pompeii aimed at providing information for the safety and retrofitting of walls and frescoes. The scope of this investigation was the detection of cracks and the survey of the inner core of masonry walls and the identification of detachments of frescoes. For the first target, GPR and seismic tomographies have been employed; for the second one, we used GPR and IRT. For both the case studies, and in particular for the masonry, the study of the constructive characteristics, proved to be very important for the interpretation of results.

## **29.2 Pompeii: History, Conservation Issues, and the Study Area**

### **29.2.1 Historical Setting**

Pompeii is one of the largest archaeological areas and most visited cultural heritage sites in the world. Its peculiarity is given by the extraordinary state of integrity of the buildings, which make possible to have a clear vision about how common people lived in ancient times. This appearance is the heritage of the volcanic eruption of Mount Vesuvius, which if on one hand caused the end of Pompeii and the death of most of its inhabitants, on the other hand, thanks to the volcanic cover of ash and pumice, made possible the preservation of the city's structures.

The foundation of Pompeii dates back to the seventh to sixth century BCE. It came under the domination of Rome in the fourth century. With the expansion of the Roman republic, which ended with the Second Punic War (218–202 BC), begins the development of the Pompeii that we know, with its streets, public buildings, and houses discovered by the first archaeological excavations conducted under the reign of Charles of Bourbon in 1748 (Fiorelli 1875). The city of Pompeii was directly involved in the great changes caused by the Roman expansionist policy, projected toward the conquest of the entire Mediterranean basin. The city enjoyed a period of prosperity and wellness obscured, however, by the social wars that destabilized the whole region.

The event that inevitably links the history of Pompeii to historiography and the collective scenario is undoubtedly the eruption of Vesuvius in 79 AD. After the eruption, the Emperor Titus immediately organized emergency assistance to coordinate the necessary aid to the reconstruction of Pompeii. However, the thick layers of ash covering Pompeii did not allow its reconstruction and the return of the population.



The rediscovery of Pompeii happened in 1748 in the age of King Carlo of Borbone when a Spanish military engineer unearthed intact buildings and wall paintings, immediately arousing the interest of scholars and intellectuals all over Europe.

Since then Pompeii has had a long and intense history of studies, surveys, excavations, and discoveries, becoming an important place not only for knowledge of Roman culture but also for the development of modern archeology.

### ***29.2.2 Pompeii: Toward a Systematic Approach to Its Conservation***

The modern history of Pompeii has been also marked by damage and destruction caused by earthquakes and bombing during WW II (Garcia 2006). Recently, constant and frequent collapses have occurred as the outcome of the difficulty of coping with systematic maintenance with the problems of degradation of materials and structures caused by weathering affecting exposed archaeological structures, the poor compatibility and effectiveness of consolidation work based on concrete made in the twentieth century, and, finally, the impact of tourism.

Following approval by the European Commission of the Great Pompeii Project, the Italian Ministry of Heritage and Culture has developed a multi-annual action plan aimed at addressing in a systematic way the issues of preservation and enhancement of the archaeological area. The Great Pompeii Project primarily aims at solving in a systematic way the issue of conservation by adopting an approach based on (1) extensive and detailed knowledge of archaeological, historical, and structural data, aimed at timely identification of risk factors and (2) systematic planning of conservation interventions and the strengthening of management capacity and scheduled periodic intervention. In particular, the plan of knowledge, through a periodic monitoring of the state of conservation of archaeological structures, is conceived as a tool for support the planning, in an effective and timely manner, of conservation and retrofitting works necessary for the prevention of traumatic events, which can lead to irreversible loss of archaeological evidence.

To this aim it is fundamental to use in an operational way all the available technologies and procedures for the diagnosis of decay pathologies to support decision making for the design and execution of restoration work. This strategy is applied at Regio (Region) VIII, where an extensive investigation campaign has been conducted by using direct surveys, in situ noninvasive tests, and laboratory analyses.

Only a small part of this experience at Regio VIII is shown here. According to the theme discussed in the first paragraph, this chapter considers the approach based on noninvasive site investigation to detect and map nonvisible decay pathologies such as cracks and fractures inside masonry and the detachment of plaster and frescoes. For the sake of brevity, only the results of investigations performed on a wall of the Basilica and frescoes in the Gymnasium are shown and discussed.

### 29.2.3 Study Area: Regio VIII, Basilica, and Gymnasium

The urban fabric of Pompeii was divided into nine regions or *Regio* by the archaeologist Fiorelli in the 1860s (Fiorelli 1875). Each regio in its turn contains a number of blocks of buildings bounded by roads, named *insulae*. One of the largest regions (*regiones*) is Regio VIII, divided into seven insulae. It occupies the southwestern sector of the urban area and is bounded (on the south) by an irregular stretch of city walls between the two gates, Porta Stabia and Porta Marina (Fig. 29.1).

Regio VIII includes a number of (1) public palaces and spaces such as the Triangular Forum, Basilica, Comitium, the theatre, and the Odeon; (2) religious buildings such as the Sanctuary of Athena and Hercules, Sanctuary of Venus, and Temples of Aesculapius and Isis; and (3) significant private houses such as domus of Championnet, domus of the Geometric Mosaics, and the houses of the Corneli.

The investigated monuments herein shown are in the Basilica and Sarno baths (Koloski Ostrow 1990; Ioppolo 1992) (Fig. 29.1)

The Basilica is dated back to 130–120 BC and is one of the oldest examples of Roman basilica. It is located in the southwest corner of the Foro and was used to carry out business and for the administration of justice. The Basilica has a rectangular plan with dimensions of about  $67.50 \times 25 \text{ m}^2$  and is divided into three naves by two rows of columns having Ionic capitals and presenting a brickwork trunk with grooves obtained by brick. The walls are made in *opus incertum* and plastered externally, whereas the inner walls were decorated in I Stile<sup>1</sup>, with stucco in relief.

The Sarno baths consist of a block of four levels built in the second century BCE. Severely damaged by the earthquake of 62 AD, the thermal rooms were still being renovated at the time of the eruption. The most significant rooms are the *Frigidarium*, decorated by paintings representing the Sarno River (from which comes the name of Sarno Bath) and Nilotic landscapes, and the *gymnasium* (Fig. 29.1, bottom), which occupies most of the complex, with frescoes depicting athletes and fight scenes dated to 50 AD (Koloski Ostrow 1990).

---

<sup>1</sup>The evolution of Pompeian painting is distinguished in four periods, each one characterized by a distinct style by the German archaeologist August Mau (1900). The first style, known also as an encrustation or masonry style, dominated a period between 200 BC and 80 BC. It is characterized by the *simulation* of some materials such as marble and architectural elements such as wooden beams, white cornices and pillars, and the use of vivid colors. The second style, also referred to as illusionism or the architectural style, was most popular in the first century BCE. It is characterized by the use of *trompe l'oeil* compositions to create the *optical illusion* of three-dimensional objects, architectural elements, and landscapes. The third style, or ornate style, was popular in the last two decades of the first century BCE. It developed as a reaction against the austerity of the second style. Fourth-style paintings depict large-scale narrative scenes and panoramic views.



**Fig. 29.1** Plan of Regio VIII (*top*), three-dimensional (3D) model of Basilica (*middle*), with indication of the investigated area: southern wall of Basilica (indicated with *dashed quadrangular light blue box*) and wall paintings in the Gymnasium in Sarno Baths (*red box*). *Bottom*: detail of the wall paintings

## 29.3 Investigations of Basilica Masonry Structures

### 29.3.1 Building, Materials and Techniques

Some walls in *opus incertum* on the southern side of the Basilica have been investigated by GPR and sonic tomography (Fig. 29.2, bottom left) with the aim to evaluate the state of conservation of the masonry, including the detection of possible cracks, fractures, and voids. Before carrying out the noninvasive investigations, several surveys have been conducted with the aim to provide the geometry of the walls, identify possible deformations, and to obtain detailed ortho photographs useful to study the building techniques. The 3D geometry of the walls has been obtained by processing and integrating terrestrial and aerial images taken from a drone by using structures from motion-based software. In this way, it has been possible to establish that the walls do not exhibit significant out-of-plane deformations.



**Fig. 29.2** *Top*: Digital model of southern wall of the Basilica investigated by GPR and seismic tomography. The wall is interrupted by plastered fluted semicolumns built with bricks. *Bottom left*: GPR data acquisition. *Bottom right*: Detail of the masonry composed of irregular stone elements of Peperino

The investigated wall, interrupted by plastered fluted semicolumns, has a thickness of approximately 0.65 m and is partially plastered with mortar composed of pozzolana and sand (Fig. 29.2, upper). The wall is composed of three layers, among which the central one (about 30 cm thick) is sufficiently connected with two adjacent ones about 15 cm thick. The external layers are built by using irregularly shaped and randomly placed first-sized or uncut tuff blocks of dimensions ranging from 12 to 18 cm (Fig. 29.2, bottom right). The central nucleus is also composed by irregularly shaped and randomly placed uncut tuff blocks of dimensions ranging from 8 to 14 cm.

The volcanic tuff named Peperino has a trachytic composition consisting of black crushed and elongated slag, immersed in a grayish cineritic matrix. The mass is entirely lithified by welding and neoformation of feldspars. It presents very variable characteristics as a function of the amount of slag.

The petrographic study<sup>2</sup> allowed establishing that the mortars were prepared with air lime mixed with aggregate, including sand and gravel, of both volcanic and local origin, belonging to volcanoclastic deposits of the Somma-Vesuvio, probably reworked by streams (alluvial deposits). The main mineralogical constituents of the aggregate constituents are related to two types of lava (predominantly plagioclase or mostly leucite), along with glass and/or pumice and clino-pyroxene. Secondary mineralogical components are feldspar (plagioclase and sanidine) and leucite. Finally, accessory components are olivine, biotite, and carbonate clasts (spathic calcite and calcite micritic).

### 29.3.2 GPR Data Acquisition and Processing

The GPR survey was carried out with a georadar Ris-Hi-Mod equipped with the 2000-MHz (center frequency) antennae manufactured by Ingegneria dei Sistemi (IDS). The selection of the working frequency was carried out on the basis of the resolution and investigation depth required by survey objectives. The acquisition was performed as follows: 512 samples per scan for a recording time window of 30 ns with the application of a manual gain function. To obtain a 3D GPR pseudo-representation, GPR profiles were collected with 0.33-m spacing (Fig. 29.3, top).

The quality of the raw data was improved by means of appropriate processing. Processing steps can be summarized as follows: (i) horizontal scaling (80 scans/m) to allow data interpolation in the *X*-direction; (ii) amplitude normalization, consisting of the declipping of saturated traces using a polynomial interpolation procedure;

---

<sup>2</sup>The petrographic analyses have been conducted by Giovanni Quarta and Davide Melica of CNR-IBAM.

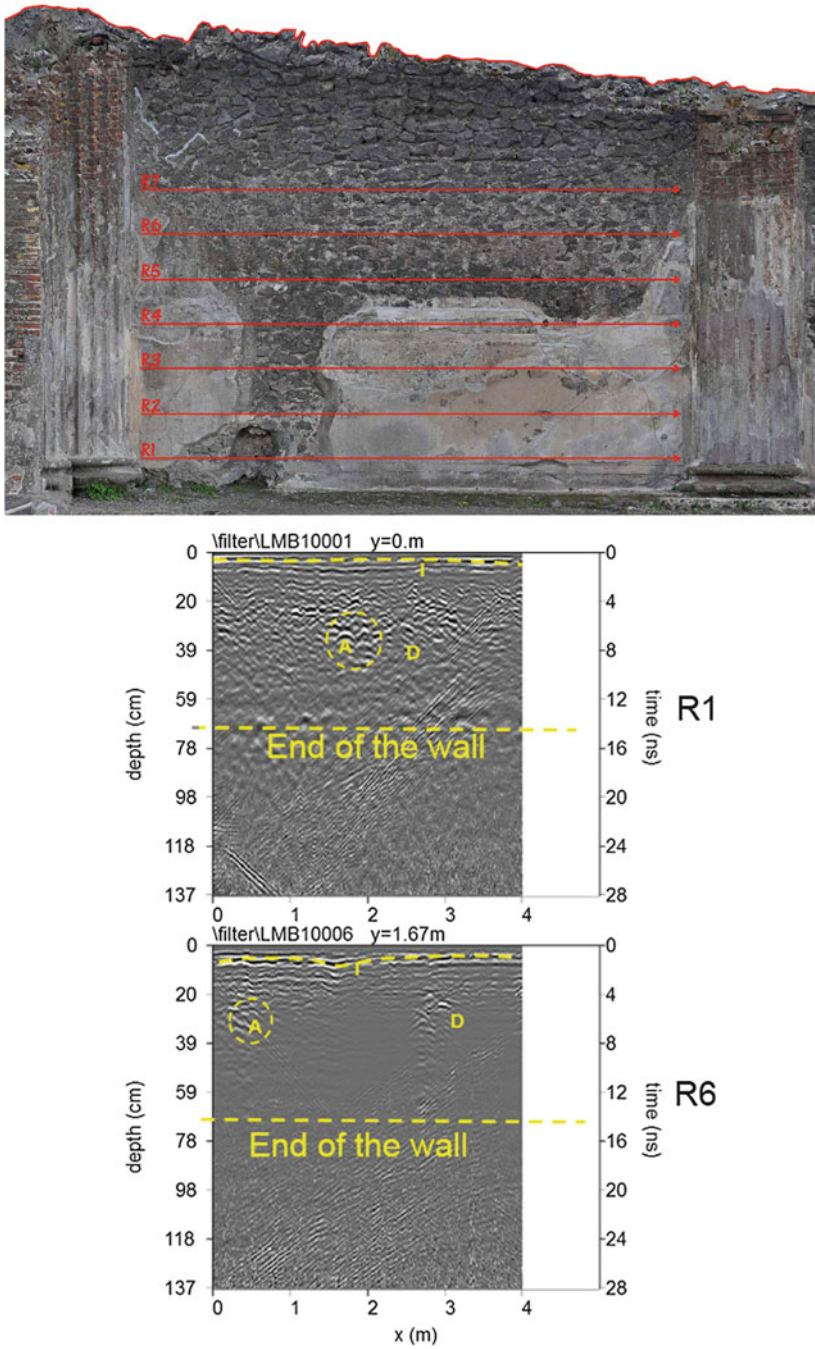


**Fig. 29.3** *Top*: Wall of Basilica: location of GPR profiles. *Middle* and *bottom*: Processed radar sections related to the profiles *R1* and *R6*

(iii) Kirchhoff 2D-velocity migration performed on the basis of a 2D-velocity distribution. The goal of the migration is to trace back the reflection and diffraction energy to their “source.”<sup>3</sup>

A good penetration of the electromagnetic energy was observed because of the low resistivity of volcanic material (Russell and Stasiuk 1997) used to build the masonry. In fact, at about 15 ns (corresponding to a thickness of about 0.65 m when the mean velocity value of 0.086 m/ns is used) it is possible to detect the end of the wall (Fig. 29.3, middle and bottom).

For sake of brevity, only the results obtained on 4 m of the southern wall of Basilica are shown (see Fig. 29.3, middle and bottom). The observation of radargrams points out the presence of reflectors for all the 15 ns corresponding to the thickness of the investigated wall. In particular, in radargrams R1 and R6 a slightly undulating reflection is present (labeled *I* in Fig. 29.3, middle) and clearly identifiable at time ranging from about 0.5 to 1.0 ns (0.02 m–0.05 m thick). Because of its high amplitude, denoting a strong electromagnetic contrast, this reflection has been interpreted as resulting from a more compact layer associated with the plaster contact.

At about 4–5 ns, corresponding to 15–20 cm, horizontal/slightly undulated reflections result from the interface between the external masonry layer (of about 15 cm) and the central layer. The undulating pattern of the reflecting surface is caused by the morphological characteristics of the masonry composed of irregularly shaped tuff and randomly placed on mortar beds.

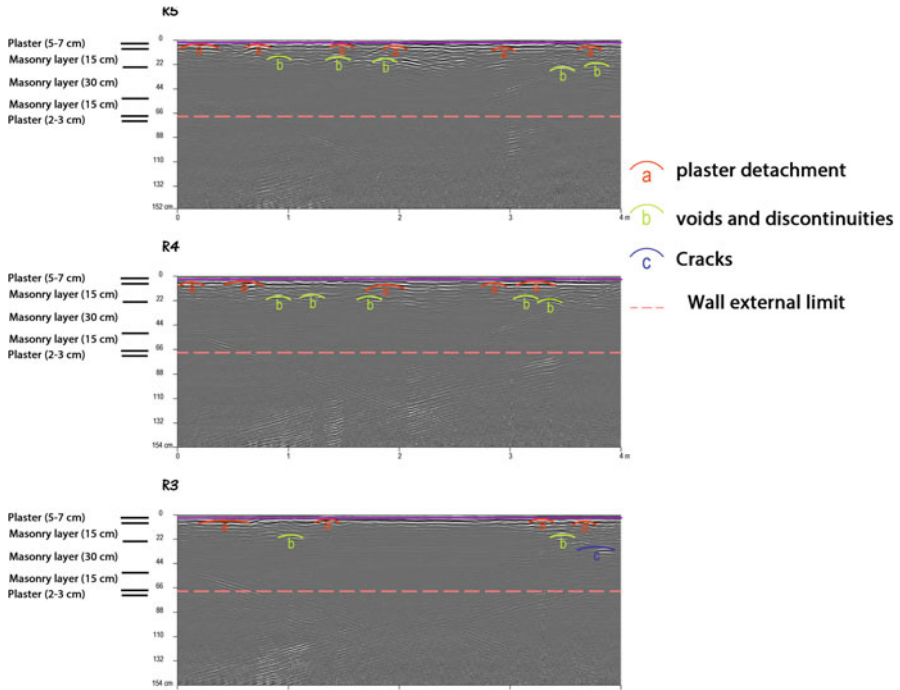
Hyperbolic reflections (labeled A in Fig. 29.3) are associated to voids present inside the wall. They are located in several positions along the  $x$ -axis but seem to have the same depth (about 0.25 m) in the wall. This interpretation was related to the fact that is clearly evident a polarity change in the single radar trace. The anomalies labeled “D” indicate possible discontinuities. These anomalies confirm an irregular pattern most likely associated with the internal arrangement of uncut or first-sized tuff block.

Figure 29.4 shows three other radargrams with an interpretation of the reflections. The reflectors are referable to three different causes: detachment of plaster (labeled with a), voids and discontinuities between the two constructive layers (labeled with b) and cracks (labeled with c) in the central layer.

A way to obtain easily interpretable maps for understanding the plan distribution of reflection amplitudes is the creation of horizontal time slices (Conyers and Goodman 1997). This data representation is important in GPR investigations as it allows an easier correlation of the most important anomalies found in the area at the same depth (Conyers 2012). Because of possible velocity changes across the

---

<sup>3</sup>The Kirchhoff two-dimensional (2D)–velocity migration is done in the  $x$ – $t$  range, which means that a weighted summation for each point of the profile over a calculated hyperbola of preset bandwidth is performed. The GPR data processing was performed used GPR-slice software (Goodman 2013).



**Fig. 29.4** Radargrams R3–R5 with interpretation of the results. Letters *a*, *b* and *c* denote reflections associated with plaster detachment, voids, and discontinuities and cracks, respectively. *Dashed pink line* indicates the wall external limit

investigated area and with depth, horizontal time slices can be considered only approximate depth slices. As underlined by several authors (e.g., Conyers and Goodman 1997), ideally the datasets for time slices should be derived from parallel profiles with a minimum spacing. Transect spacing should be less than one half the wavelength of possible reflections returned from the smallest target to be mapped: the transect spacing was 0.15 m. Assuming a 2000-MHz central frequency, the criterion of half the wavelength implies a transect spacing of 0.021 m. In theory, this should preclude the use of time slicing on these data. The effective target area is measured by the radius of the Fresnel zone.

For the surveyed area in a medium of dielectric permittivity of 12 and at depth of 0.65 m, this gives the theoretical target areas of about 0.24 m. As the anomalies lie within 0.65 m of the wall surface, the resolution of time slices constructed from profiles taken at 0.15-m intervals will be near the optimum. Time slice maps are built averaging the amplitude (or the square amplitude) of the radar signal within consecutive time windows of width  $\Delta t$ . In the investigated walls of the Basilica in Pompeii, the time slice technique has been used to display the amplitude variations



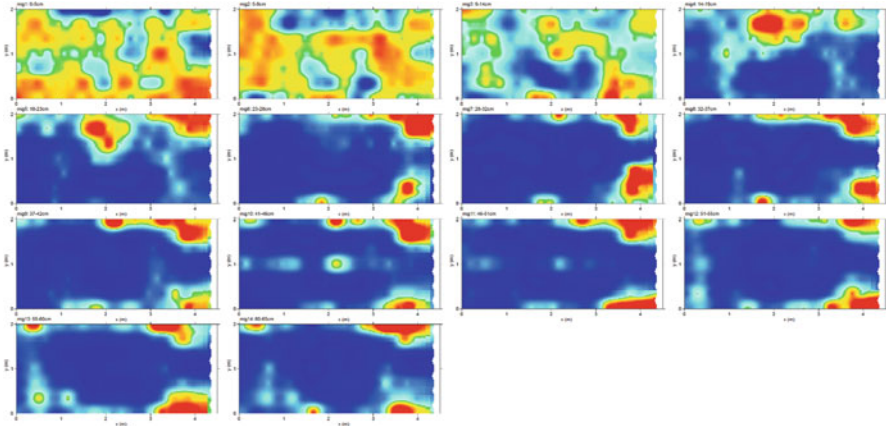


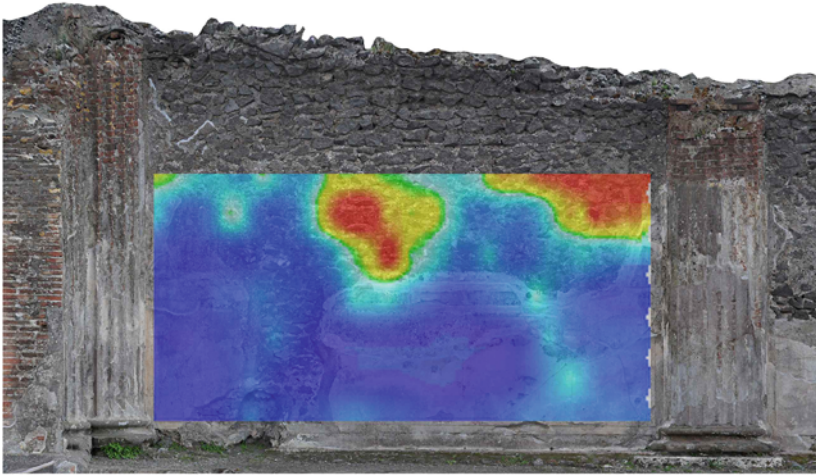
**Fig. 29.5** The Basilica walls: depth slices

within overlay time windows of width  $\Delta t = 1$  ns. The selected two-way time interval corresponds to a wall layer, approximately 0.04 m thick, and the time slices are located between 0 and 0.65 m in depth. The slices shown in Fig. 29.5 were obtained using the processed data. Several events are visible as high-amplitude anomalies. All anomalies are discontinuous and related to the presence of cracks and voids.

Figure 29.6 shows two time slices selected at the depths of 18–23 and 46–51 cm, both of them close to the interface between the wall central layer and the external layer. Comparing the two time slices with the radargrams in Fig. 29.4, it is possible to establish that the high-amplitude anomalies are associated to local discontinuities, which do not ensure an effective connection between the three masonry layers.

Another approach for visualizing 3D radar data has been proposed by Conyers (2004, 2012). In this case, after an appropriate processing of radar data, a 3D image of the diffracting or reflecting object can be easily obtained by (i) extraction of a particular complex signal attribute (trace envelope), the grid data are converted to the reflection strength or amplitude envelope thanks to a Hilbert transformation; and (ii) thresholding (a threshold value must be entered). Hence all amplitudes greater/equal than the threshold value are considered per definition; (iii) 3D contouring by means of iso-amplitude surface. As pointed out by Conyers (2004), in this case the choice of the threshold is a crucial task. Figure 29.7 depicts the same data set with iso-amplitude surfaces using a threshold value of 60% of the maximum complex trace amplitude. Obviously, lowering the threshold value, increases the visibility of the main anomaly and smaller objects, but also heterogeneity noise. A relatively strong continuous reflection is visible on the threshold volumes (between 0.02 and 0.65 m). This visualization technique points out better the damaged zone.

GPR time slice at 18-23 cm depth



GPR time slice at 46-51 cm depth

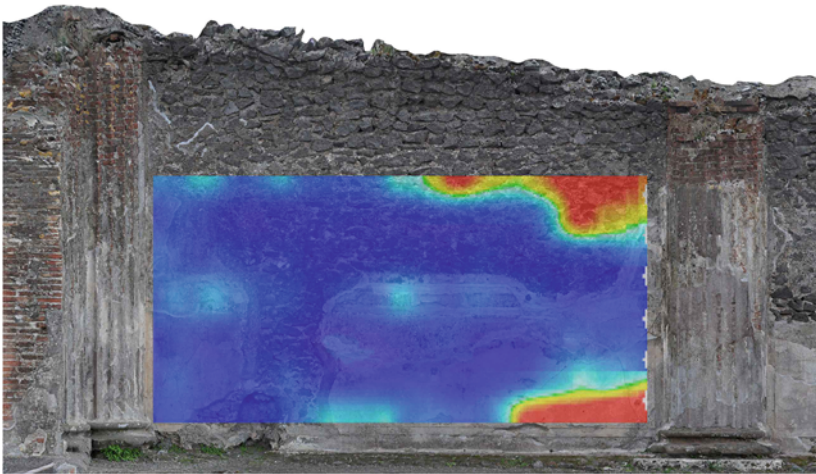
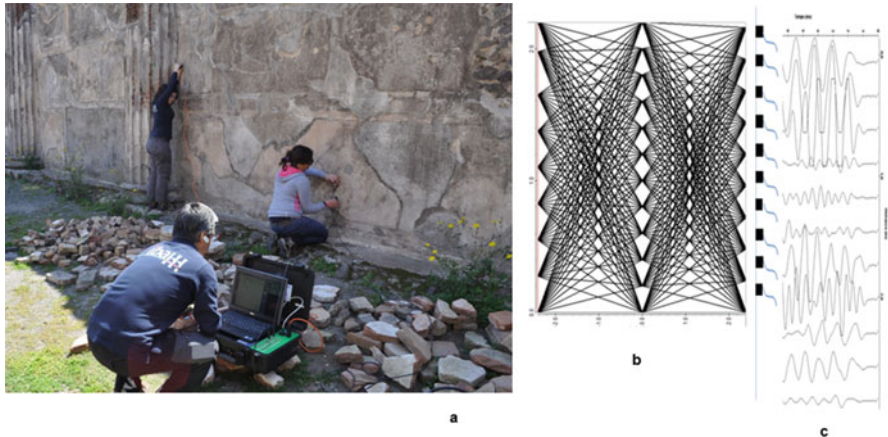
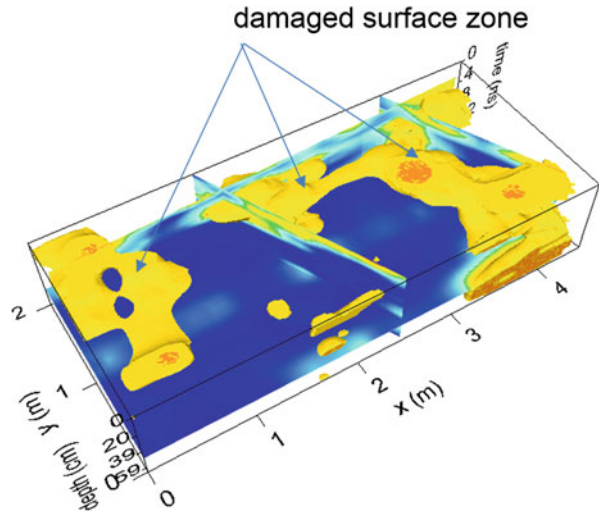


Fig. 29.6 GPR time slices at depths of 18–23 cm and 46–51 cm

### 29.3.3 *Seismic Tomography Data Acquisition and Analysis of the Basilica Walls*

Seismic tomography of the Basilica walls consisted of 3D reconstruction based on the travel-refracted wave amplitude. Images were obtained from the first arrival of the waves. Data were acquired obtained along the 4 m × 2 m area (Fig. 29.8a).

**Fig. 29.7** The Basilica walls: iso-amplitude surfaces using a threshold value of 60%



**Fig. 29.8** The Basilica walls: seismic tomography. (a) Position of the accelerometers on the wall. (b) Ray paths in a hypothetic homogeneous wall. (c) Seismogram

A piezoelectric pulse at 55 KHz was used as the seismic source. Data were acquired with a high-frequency sensitivity accelerometer (55 KHz).

To cover the whole space, the medium has been divided into cells or elements, and the results are obtained as the sum of the values in each of the cells. In the case of nonhomogeneous media, the seismic wave is refracted because of changes in the wave velocity associated with adjacent cells, and the tomography equations are solved in an iterative computational process until a reliable and accurate solution is attained. The computational process, the simultaneous interactive reconstruction

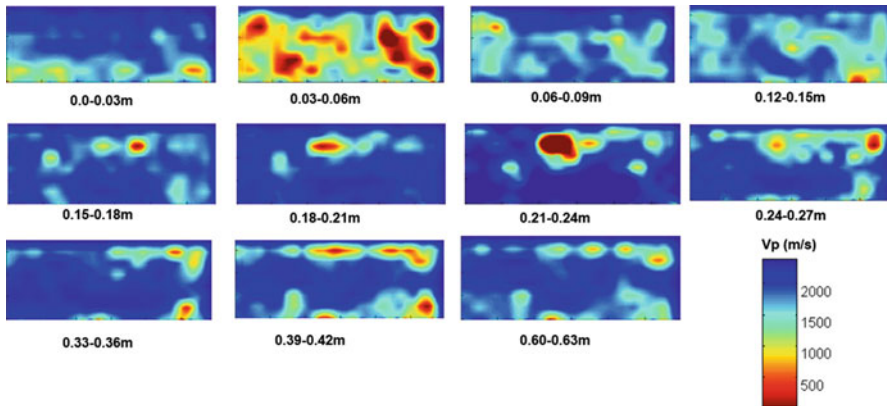


**Fig. 29.9** The Basilica walls: P-wave velocity distribution at several depths in the wall

technique (SIRT), contemplates ray curvature as a consequence of internal refractions. The characteristics of each cell are defined in the case that at least one ray path crosses the cell (Fig. 29.8b, c). The Reflex software was used for the inversion of the seismic data.

Seismic tomography seems to confirm the existence of discontinuities and voids. Several zones of the depth slices presenting lower velocities (400–500 m/s) could be associated with cracks or more damaged parts of the wall (Fig. 29.9). These low-velocity zones are usually located close to the wall surface or in the shallowest part of the wall. The depth of 0.21–0.24 m, in correspondence with the interface between external and central masonry layers, is characterized by the lowest P-wave velocity values (about 250–350 m/s); this indicates the probable presence of voids and consequently the lack of connection between the two wall layers. Such a hypothesis is confirmed by a GPR time slice at 0.18–0.23 m: in fact, the areas of the wall exhibiting low P-wave velocity values are also characterized by high-amplitude GPR (see Fig. 29.10). This behavior can be observed at the top center and upper right of the wall (Fig. 29.10).

Irregular and small changes on the velocity are most likely caused by the irregular arrangement of materials inside the structure. However, it is noticeable that the wall exhibits high inhomogeneity. Low P-wave velocity values are also found at depths of 0.39–0.42 m (see Fig. 29.11, top), also corresponding, in this case, to high-amplitude GPR (Fig. 29.11, bottom), and consequently referable to voids and discontinuities between wall layers.

The case study just discussed demonstrates the importance of integrating different diagnostic techniques, such as GPR and seismic tomography, to infer reliable information about the presence of degradation pathologies.

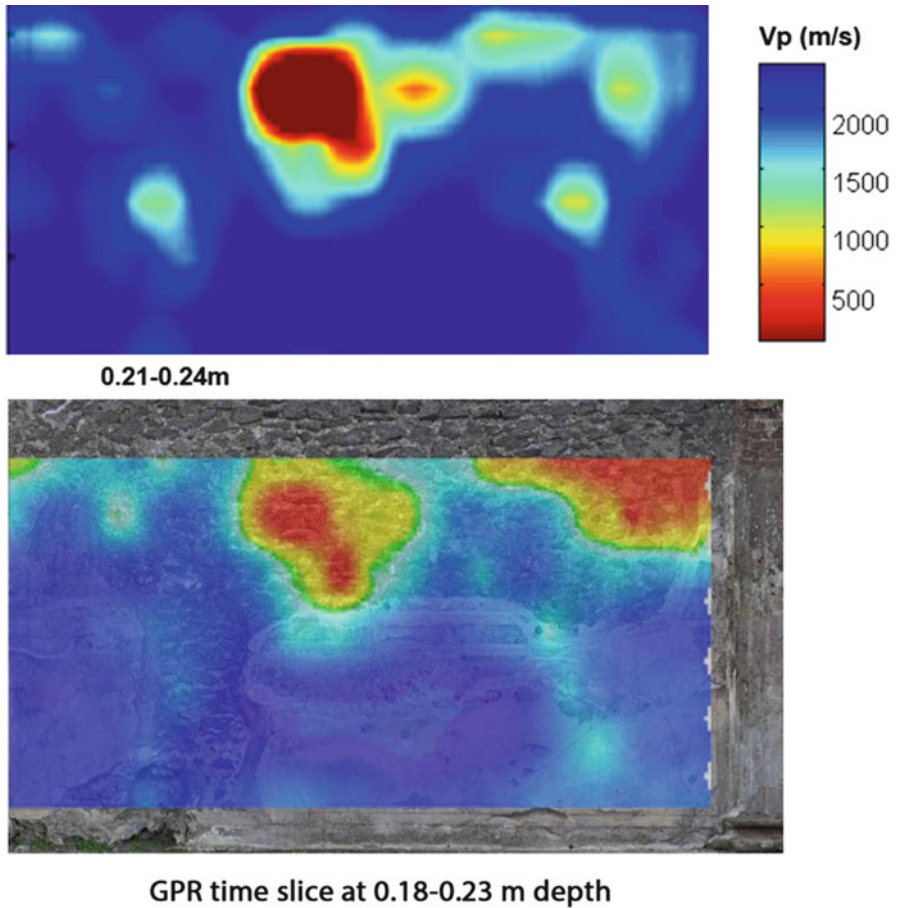


**Fig. 29.10** Comparison between P-wave velocity distribution at depths of 0.21–0.24 m (*upper*) and GPR time slice at depths of 0.18–0.23 m (*bottom*). The high-amplitude GPR corresponds to low velocity values, confirming the presence of voids and discontinuities between the central nucleus and the external layer of the wall

## 29.4 Conservation Assessment of the Fresco of Sarno Baths by GPR and IRT

### 29.4.1 Introduction

The knowledge of Roman painting is mainly derived from the unique conditions of preservation of Pompeii and the other Vesuvian cities of Herculaneum and Stabia,

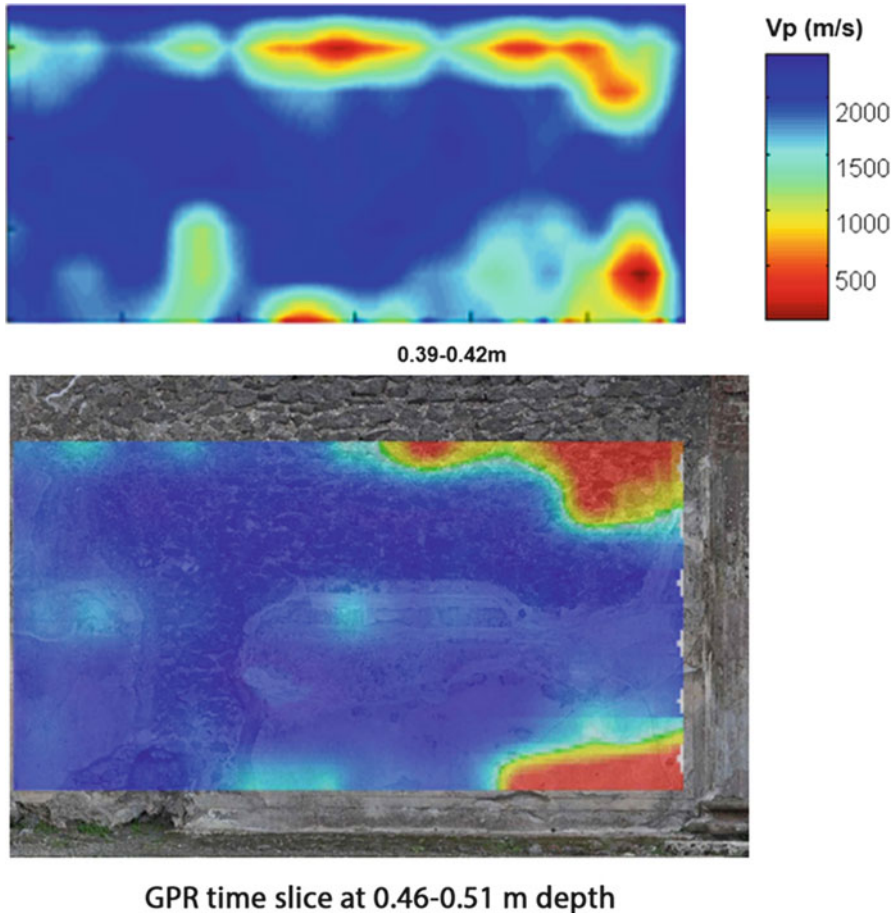


**Fig. 29.11** Comparison between P-wave velocity distribution at 0.39–0.42 m depth (*up*) and GPR time slice at 0.46–0.51 m depth (*bottom*)

where huge quantities of wall paintings have been discovered. Pompeian paintings are dated between the second century BC and 79 AD, the eruption date.

Pompeian wall paintings were done in fresco, tempera, and encaustic. The frescoes were done on plaster of fresh lime with ground pigments diluted in water. Tempera painting was performed by diluting the colors with sticky and gummy solvents, such as egg yolk, and the wax. Finally, the encaustic painting was achieved with colors mixed with wax.

Although 80% of the wall paintings in Pompeii have been detached, applied to a new support, and conserved in museums, there are still several paintings in the ruins

of Pompeii and most of them need conservation treatment and restoration, because these are affected by delamination (or detachment), flaking, disruption, cracks and hatching, and mechanical damage.

Delamination is the most common cause of deterioration of frescoes because such works of art were originally created using a complex construction technique based on different plastering sequences. In addition, the 'original' heterogeneity is worsened by the differential nature of the materials used in restoration.

On the basis of the direct observation of investigated frescoes and from the scientific literature, the plaster stratigraphy of wall painting in Sarno Baths seems to be composed of three layers.

The deepest plaster is the so-called *arriccio*, 3–4 cm thick, the function of which is to cling to the wall and provide a good moisture reserve for the overlying layers. The second layer (1–1.5 cm thick) is composed of gray-colored sublayers (inserted 'wet to wet') made up of a lime binder with an aggregate containing black volcanic sand and lumps of calcareous material. The under sublayer of plaster is slightly coarser than the upper layer. Finally, there is the '*intonachino*,' which is a thin white plaster layer consisting of a lime binder with crystalline calcite as one of the aggregates.

#### ***29.4.2 Noninvasive Investigations on Frescoes by GPR and IRT***

Two walls of the Gymnasium of the Sarno Baths (located in *Insula* 2 of *Regio* VIII) have been investigated by using GPR and IRT with the aim to evaluate the state of adherence of plaster layers and other possible features referable to decay pathologies of wall painting.

Before GPR and IRT inspections, an architectural survey was performed by structure-from-motion photogrammetry, by processing multiple photographs with a large overlap. In this way, orthophotographs and digital models of the wall paintings were achieved whose details allowed us to map decay pathologies of paintings. Figure 29.12 shows the 3D visualization of the two wall paintings located at South and East, respectively. The 3D mesh and textured models (Fig. 29.12: upper and bottom, respectively) indicate the lack of the external layer of fresco as well as other decay pathologies such as deposits, biological patina, and efflorescence (salt coating).

For sake of brevity we discuss only the results obtained from GPR and IRT investigations on one of the two investigated wall paintings, in particular, the largest one (south wall), shown in Fig. 29.13.

The GPR survey was performed with the Hi-Mod GPR of IDS using the antenna at 2-GHz frequency. The GPR antenna was moved on the painted surface by using a plastic panel against the wall. GPR data were collected with 512 samples per scan for a recording time window of 30 ns and a manual gain function. The survey was carried out in continuous mode along 0.2-m spaced parallel profiles in the part of

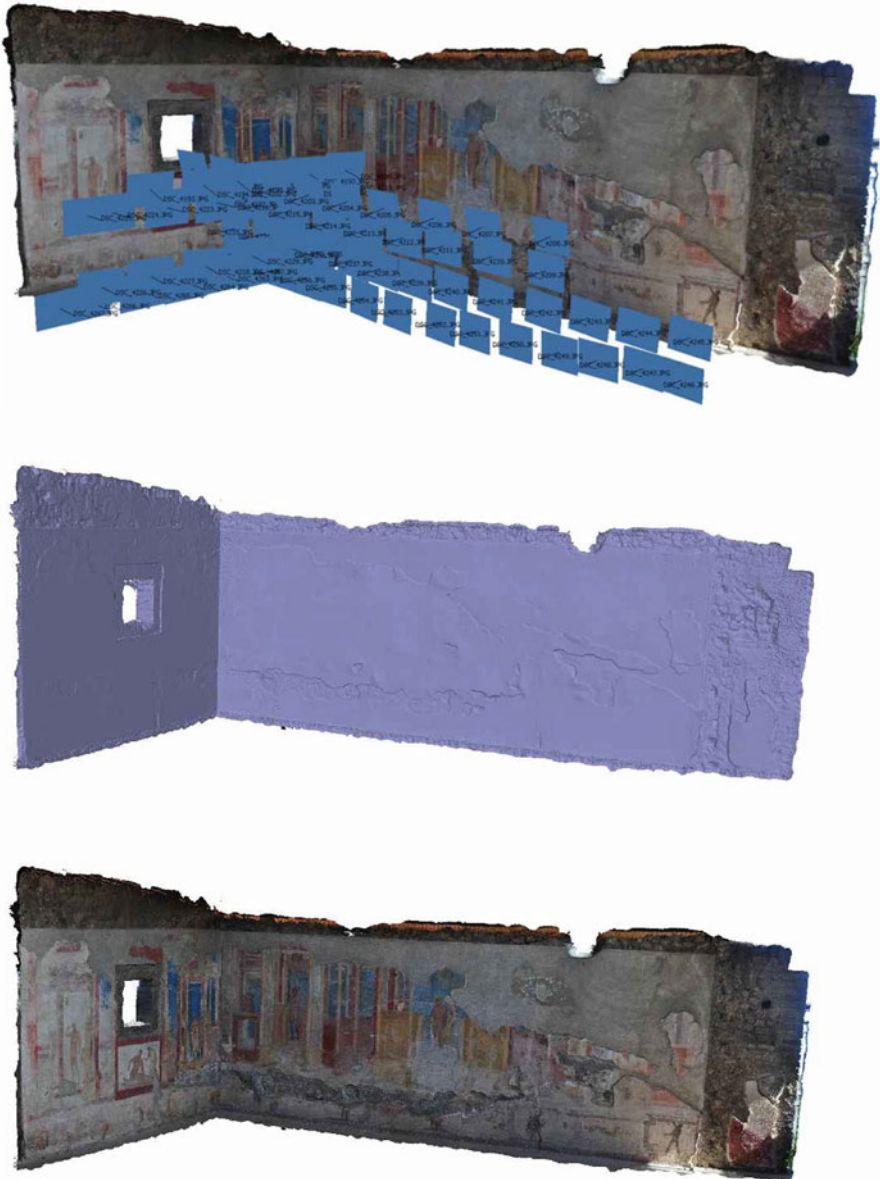


**Fig. 29.12** 3D mesh and textured model of the wall paintings in the Gymnasium

the fresco less damaged (dimensions of the surveyed area,  $1\text{ m} \times 5\text{ m}$  from  $1\text{ m}$  in height above the floor), which allowed an optimal contact of the georadar with the wall painting. The velocity value for the electromagnetic wave was estimated as equal to  $0.10\text{ m/ns}$ .





**Fig. 29.13** The Gymnasium: Orthophotograph of the south wall painting. The *black rectangular box* denotes the area of fresco investigated by GPR

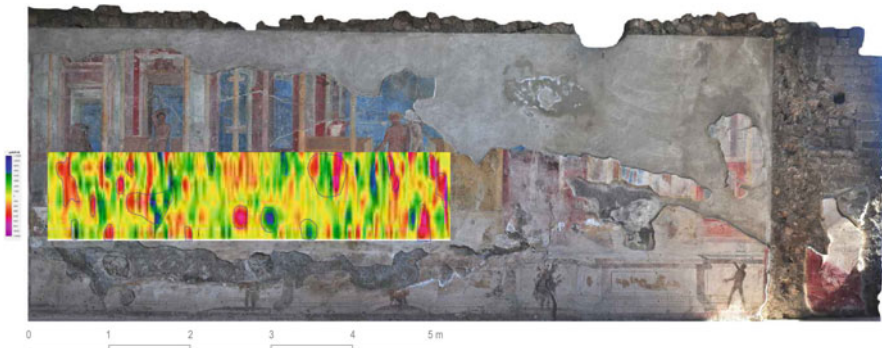


**Fig. 29.14** The Gymnasium: Detail of the wall painting with GPR time slice at 4.7 cm depth. *Light blue lines* border areas characterized by high amplitude

To obtain further information on the presence of discontinuity, appropriate processing has been performed for easier interpretation. Processing steps can be summarized as follows:

- Background removal procedure (Persico and Soldovieri 2008) for the filtering of the wall interface response
- Declipping to eliminate local saturations in amplitude of the traces followed by an interpolation procedure for the reconstruction of the saturated waveforms
- Kirchhoff migration by adopting the velocity of EM wave equal to 0.10 m/ns
- Low-pass filtering that deletes high-frequency noise present in radar scans

GPR-processed data show few reflectors, likely associated with nonperfect adhesion of the plaster to the wall in a depth range 1–5 cm.

The highest values of radar amplitude are observed at the depth of 4.7 cm in correspondence to the interface between the plaster (the third layer, the deep *arriccio*) and the wall (see Fig. 29.14). Other significant values of radar amplitude

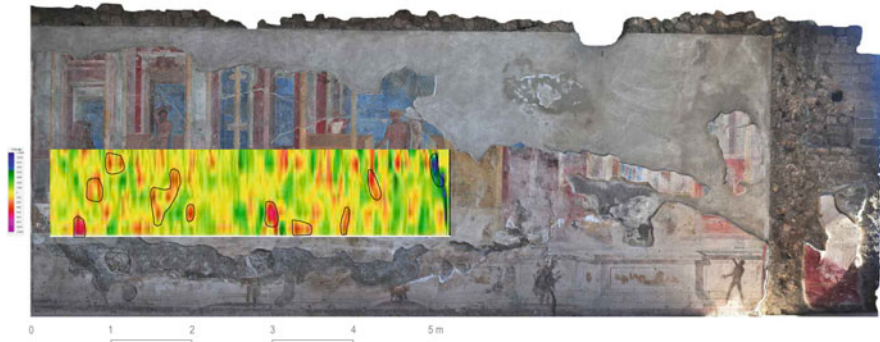


**Fig. 29.15** The Gymnasium: Detail of the wall painting with GPR time slice at 3.5 cm depth. *Black lines* border areas characterized by high amplitude likely referable to detachment between two plaster layers (arriccio and deep arriccio)

are at a depth between 2 and 3 cm near to the interface between ‘arriccio’ and ‘deep arriccio’ (see Fig. 29.15).

The entire wall painting has been also investigated by IRT with the aim to provide complementary data for facilitating the interpretation of GPR results. In particular, the main interest has been that to verify the presence of thermal anomalies in correspondence with the GPR signal of high amplitude.

IRT prospections have been performed by using the passive method in an indoor environment. IRT images were collected with a FLIR SC660 sensor FPA (Focal Plane Array) uncooled microbolometer operating in the spectral range between 7.5 and 14  $\mu\text{m}$ . The identification of thermal anomalies depends on the surface characteristics of emissivity and roughness and on the physical properties of the materials. In this way, information is gained about the thickness, type, and state of preservation of the plaster.

Despite the low natural heating, the thermal maps exhibit few spatial temperature changes, which can be associated with salt coating, patina, and deposits; other more significant thermal anomalies are referable to possible problems of detachment or sparse adherence between plaster layers (Fig. 29.16).

The integration and fusion of GPR and IRT methods (see Fig. 29.17) provided a map of possible areas of interest likely referable to decay pathologies or inhomogeneities in the multi-layered structure of the frescoes.

In particular, the matching between GPR reflectors and thermal anomalies could be reasonably considered an indicator of detachments or scarce adherence between plaster and wall or of problems of delamination between the plaster layers.

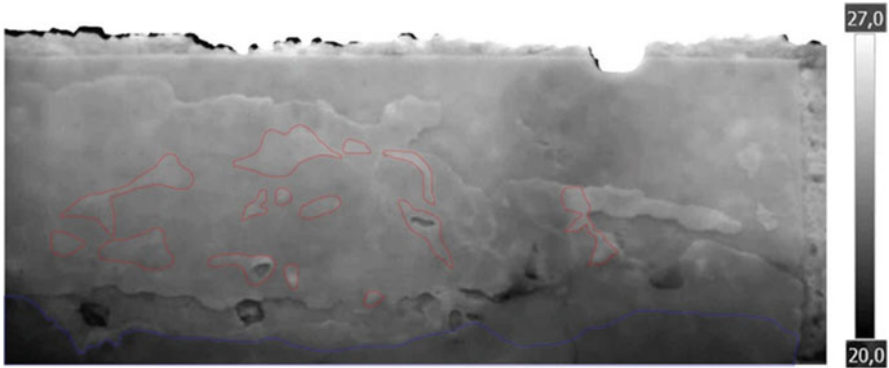


**Fig. 29.16** The Gymnasium: Detail of IRT image of the wall painting. *Red lines* border areas characterized by thermal anomalies likely referable to detachment. *Blue lines* indicate areas affected by rising damp



**Fig. 29.17** The Gymnasium: Detail of the wall painting. *Black and light blue lines* border areas characterized by high-amplitude GPR at 3.5 and 4.7 cm depth, respectively. *Red lines* border areas characterized by thermal anomalies. *Blue lines* indicate areas affected by rising. The images show that most of the thermal anomalies are characterized by GPR at high amplitude at 3.5-cm depth, likely resulting from the presence of detachment or scarce adherence between the plaster layers of the fresco

## 29.5 Conclusions

This chapter has presented two interesting cases of integration among noninvasive diagnostics techniques in the framework of work of restoration of the *Regio VIII* in the Pompeii.

The first study case is concerned with the detection of cracks and the collection of constructive features of masonry structures, whereas the second is related to the identification and survey of fresco detachment.

For the first study case, GPR and seismic tomographic methods were integrated for the diagnosis of walls in *opus incertum* on the southern side of the Basilica. The main outcome of this survey was the evaluation of the state of conservation of masonry, including the detection of possible cracks, fractures, and voids. Before carrying out the GPR and seismic investigations, several surveys were conducted to provide the geometry of the walls, identify possible deformations, and to obtain detailed orthophotographs useful to study the building techniques. The 3D geometry of the walls has been obtained by processing and integrating terrestrial and aerial images taken from a drone. In this way, it has been possible to establish that the walls present significant cracks and discontinuities in the masonry but do not exhibit out-of-plane deformations.

The second test case was concerned with fresco investigation at two walls of the Gymnasiun of Sarno Baths (located in insula 2 of Regio VIII). In this case, the joint use of GPR and IRT permitted gaining information about possible detachments or scanty adherence between plaster and wall or problems of delamination between the plaster layers. The integration was based on the spatial correlation of the GPR and thermal anomalies, and it was possible to obtain a map of areas affected by decay pathologies or inhomogeneities in the multi-layered structure of the frescoes.

**Acknowledgements** The present publication is based on the results of non invasive investigations performed in 2015 by CNR\_IBAM, funded by Samoa srl, for the restoration of Regio VIII.

**Author Contributions** N. Masini conceived the study. N. Masini and M. Sileo wrote the paper, with the contribution of G. Leucci for paragraphs 29.3.2, 29.3.3 and 29.4.2, and A. D'Antonio for the study area (paragraph 29.2). F. Soldovieri reviewed the manuscript. GPR and seismic data have been acquired by G. Leucci, L. De Giorgi and M. Sileo. Leucci and Sileo processed GPR data. Seismic data have been processed by Leucci. Infrared data have been acquired and processed by M. Sileo. The terrestrial surveys has been performed by M. Scavone, A. Pecci and A. D'Antonio, the UAV-based surveys has been made by A. Pecci. The interpretation of data has been done by N. Masini, G. Leucci, M. Scavone, M. Sileo.

## References

- Avdelidis NP, Moropoulou A (2004) Applications of infrared thermography for the investigation of historic structures. *J Cult Herit* 5:119–127
- Binda L, Saisi A, Zanzi L (2003) Sonic tomography and flat jack tests as complementary investigation procedures for the stone pillars of the temple of S.Nicolo' L'Arena (Italy). *NDT & E Int* 36:215–227
- Binda L, Zanzi L, Lualdi M, Condoleo P (2005) The use of georadar to assess damage to a masonry Bell Tower in Cremona, Italy. *NDT & E Int* 38(3):171–179
- Brandi C (1963) *Teoria del restauro di Cesare Brandi*. Edizioni di Storia e Letteratura, Rome
- Cardarelli E, Godio A, Morelli G, Sambuelli L, Santarato G, Socco LV (2002) Integrated geophysical surveys to investigate the Scarsella vault of St. John's Baptistery in Florence. *Lead Edge* 67:467–470
- Carlomagno GM, Di Maio R, Fedi M, Meola C (2011) Integration of infrared thermography and high-frequency electromagnetic methods in archaeological surveys. *J. Geophys. Eng* 8(2011):S93–S105

- Cataldo R, De Donno A, De Nunzio G, Leucci G, Nuzzo L, Siviero S (2005) Integrated methods for analysis of deterioration of cultural heritage: the Crypt of “Cattedrale di Otranto”. *J Cult Herit* 6:29–38
- Conyers LB (2004) Ground-penetrating Radar for archaeology. AltaMira, Walnut Creek
- Conyers LB (2012) Interpreting ground-penetrating Radar for archaeology. Left Coast Press, Walnut Creek
- Conyers LB, Goodman D (1997) Ground-penetrating Radar: an introduction for archaeologists. AltaMira, Walnut Creek
- Cosentino PL, Capizzi P, Fiandaca G, Martorana R, Messina P (2009) Advances in micro geophysics for engineering and cultural heritage. *J Earth Sci* 20:626–639
- D’Aranno PJV et al (2015) High-resolution geomatic and geophysical techniques integrated with chemical analyses for the characterization of a Roman wall. *J Cult Herit*. doi:10.1016/j.culher.2015.06.005
- Danese M, Demšar U, Masini N, Charlton M (2010) Investigating material decay of historic buildings using visual analytics with multi-temporal infrared thermographic data. *Archaeometry* 52(3):482–501
- Dumoulin J (2016) Infrared thermography: from sensing principle to non destructive testing considerations. In: Masini N, Soldovieri F (eds) *Sensing the past*. Springer, Cham
- Fiorelli G (1875) *Descrizione di Pompei*. Tipografia Italiana, Napoli
- Gabellone F, Leucci G, Masini N, Persico R, Quarta G, Grasso F (2013) Non-destructive prospecting and virtual reconstruction of the chapel of the Holy Spirit in Lecce, Italy. *Near Surf Geophys*. doi:10.3997/1873-0604.2012030
- Garcia L (2006) *Danni di guerra a Pompei. Una dolorosa vicenda quasi dimenticata*, Studi della Soprintendenza Archeologica di Pompei 15. “L’Erma” di Bretschneider, Roma
- Goodman D (2013) GPR Slice Version 7.0 Manual. <http://www.gpr-survey.com>. Accessed 28 Jan 2017
- Grinzato EP, Bison G, Marinetti S (2002a) Monitoring of ancient buildings by the thermal method. *J Cult Herit* 3(2002):21–29
- Grinzato EP, Bressan C, Marinetti S, Bison PG, Bonacina C (2002b) Monitoring of the Scrovegni Chapel by IR thermography: Giotto at infrared. *Infrared Phys Technol* 43(3–5):165–169
- ICOMOS (2003) ICOMOS Charter- principles for the analysis, conservation and structural restoration of architectural heritage. Ratified by the ICOMOS 14th General Assembly, in Victoria Falls, Zimbabwe, October 2003
- Inagaki T, Ishii T, Iwamoto T (1999) On the NDT and E for the diagnosis of defects using infrared thermography. *NDT&E Int* 32:247–257
- Ioppolo G (ed) (1992) *Le Terme del Sarno a Pompei. Iter di un’analisi per la conoscenza, il restauro e la protezione sismica del monumento*, Soprintendenza Archeologica di Pompei. *Monografie* 5. “L’Erma” di Bretschneider, Roma
- Koloski Ostrow A (1990) *The Sarno Bath Complex*. “L’Erma” di Bretschneider, Roma
- Kordatos EZ, Exharcos DA, Stavrakos C, Moropoulou A, Matikas TE (2013) Infrared thermographic inspection of murals and characterization of degradation in historic monuments. *Constr Build Mater* 48:1261–1265
- Leucci G (2016) Seismic and Sonic Applications on artifacts and historical building. In: Masini N, Soldovieri F (eds) *Sensing the past*. Springer, Cham
- Leucci G, Masini N, Persico R, Soldovieri F (2011) GPR and sonic tomography for structural restoration: the case of the cathedral of Tricarico. *J Geophys Eng* 8(3):76–92. doi:10.1088/1742-2132/8/3/S08
- Leucci G, Masini N, Persico R, Quarta G, Dolce C (2012) A multidisciplinary analysis of the crypt of the holy spirit in monopoli (Southern Italy). *Near Surf Geophys* 10:1–8. doi:10.3997/1873-0604.2011032
- Leucci G, Persico R, Soldovieri F (2007) Detection of fractures from GPR data: the case history of the Cathedral of Otranto. *J Geophys Eng* 4:452–461
- Maierhofer C, Leopold S (2001) Radar investigation of masonry structures. *NDT & E Int* 34:139–147

- Maierhofer C et al (2003) Detection of shallow voids in concrete structures with impulse thermography and radar. *NDT&E Int* 36:257–263
- Masini N, Nuzzo L, Rizzo E (2007) GPR investigations for the study and the restoration of the Rose Window of Troia Cathedral (Southern Italy). *Near Surf Geophys* 5:287–300
- Masini N, Persico R, Rizzo E (2010a) Some examples of GPR prospecting for monitoring of the monumental heritage. *J Geophys Eng* 7:190–199. doi:[10.1088/1742-2132/7/2/S05](https://doi.org/10.1088/1742-2132/7/2/S05)
- Masini N, Persico R, Rizzo E, Calia A, Giannotta MT, Quarta G, Pagliuca A (2010b) Integrated techniques for analysis and monitoring of historical monuments: the case of S. Giovanni al Sepolcro in Brindisi (Southern Italy). *Near Surf Geophys* 8(5):423–432. doi:[10.3997/1873-0604.2010012](https://doi.org/10.3997/1873-0604.2010012)
- Masini N, Gabellone F, Leucci G, Persico R, Soldovieri F (2013) Enhancement of the information content available from non invasive diagnostics for restoration and knowledge of architectural heritage. In: *Proceedings of Built heritage 2013 monitoring conservation management*, Milano, 18–20 Nov 2013, pp 824–828
- Mau A (1900) *Pompeji in Leben und Kunst*. Engelmann, Leipzig
- Meier T, Aura M, Fehr M, Köhn D, Cristiano L, Sobott R, Mosca I, Ettl H, Eckel F, Steinkraus T, Erkul E, Schulte-Kortnack D, Sigloch K, Bilgili F, Di Gioia E, Parisi Presicce C (2016) Chapter XX: Investigating surficial alterations of natural stone by ultrasonic surface measurements. In: Masini N, Soldovieri F (eds) *Sensing the past. Geoscience and sensing technologies for cultural heritage*. Springer, Cham
- Moropoulou A, Labropoulos K, Delegou E, Bakolas A (2013) Non-destructive techniques as a tool for the protection of built cultural heritage. *Constr Build Mater* 48:1222–1239
- Nuzzo L, Masini N, Rizzo E, Lasaponara R (2007) Integrated and multiscale NDT for the study of architectural heritage. In: Michel U, Civco DL, Ehlers M, Kaufmann HJ (eds) *Proceedings of SPIE, remote sensing for environmental monitoring, GIS applications, and geology VIII*, vol. 7110, p 711015
- Nuzzo L, Calia A, Liberatore D, Masini N, Rizzo E (2010) Integration of ground-penetrating radar, ultrasonic tests and infrared thermography for the analysis of a precious medieval rose window. *Adv Geosci* 24:69–82
- Pérez-Gracia V, Caselles JO, Clapés J, Martínez G, Osorio R (2013) Non-destructive analysis in cultural heritage buildings: evaluating the Mallorca cathedral supporting structures. *NDT & E Int* 59:40–47
- Pérez-Gracia V, González-Drigo R, Di Capua D (2008) Horizontal resolution in a non-destructive shallow GPR survey: an experimental evaluation. *NDT&E Int* 41:611–620
- Persico R (2014) *Introduction to ground penetrating radar: inverse scattering and data processing*. Wiley, Hoboken. ISBN:9781118305003
- Persico R, Sato M (2016) Ground penetrating radar: technologies and data processing issue for applications in the field of cultural heritage. In: Masini N, Soldovieri F (eds) *Sensing the past*. Springer, Cham
- Persico R, Soldovieri F (2008) Effects of the background removal in linear inverse scattering. *IEEE Trans Geosci Remote Sens* 46(4):1104–1114
- Ranalli D, Scozzafava M, Tallini M (2004) Ground penetrating radar investigations for the restoration of historic buildings: the case study of the Collemaggio Basilica (L'Aquila, Italy). *J Cult Herit* 5:91–99
- Russell JK, Stasiuk MV (1997) Characterization of volcanic deposits with ground-penetrating radar. *Bull Volcanol* 58(7):515–527
- Saisi A, Gentile C, Guidobaldi M (2015) Post-earthquake continuous dynamic monitoring of the Gabbia Tower in Mantua, Italy. *Constr Build Mater* 81:101–112
- Soldovieri F, Orlando L (2009) Novel tomographic based approach and processing strategies for GPR measurements using multifrequency antennas. *J Cult Herit* 10:e83–e92